Neurobiology of Aging 88 (2020) 61–70

Contents lists available at ScienceDirect

Neurobiology of Aging

journal homepage: www.elsevier.com/locate/neuaging

Cerebrospinal fluid progranulin is associated with increased cortical thickness in early stages of Alzheimer's disease

Lucia Batzu*, Eric Westman, Joana B. Pereira, for the Alzheimer's Disease Neuroimaging Initiative[1]

Division of Clinical Geriatrics, Department of Neurobiology, Care Sciences and Society, Karolinska Institute, Huddinge, Sweden

ARTICLE INFO

Article history:
Received 6 August 2019
Received in revised form 11 December 2019
Accepted 14 December 2019
Available online 20 December 2019

Keywords:
Alzheimer's disease
Progranulin
Neuroinflammation
Cerebrospinal fluid
Magnetic resonance imaging
Cortical thickness

ABSTRACT

Progranulin plays an important role in neuroinflammation in Alzheimer's disease (AD) pathophysiology, being upregulated by activated microglia. This study assessed whether cerebrospinal fluid levels of progranulin correlated with structural neuroimaging measures and cognition in 122 cognitively normal individuals, 81 mild cognitive impairment, and 70 AD patients from the Alzheimer's Disease Neuroimaging Initiative. Cognitively normal subjects were classified into 3 groups using the AT(N) system, whereas all mild cognitive impairment and AD patients were A+/TN+. Correlations between progranulin with neuroanatomical measures and cognitive decline were performed within each group. Progranulin was associated with cortical thickening in parietal, occipital, and frontal regions in cognitively normal individuals with amyloid pathology. These subjects also showed cortical thickening compared with A −/TN− subjects, an effect that was partially mediated by progranulin. In addition, higher progranulin correlated with longitudinal cognitive decline. The association between progranulin and cortical thickening, together with regional "brain swelling" in A+/TN− subjects, suggests progranulin contributes to the neuroinflammatory structural changes in preclinical AD.

1. Introduction

Neuroinflammation is one of the major determinants in the pathophysiology of Alzheimer's disease (AD), being mediated by microglial cells, astrocytes, and numerous inflammatory modulators (Eikelenboom et al., 2011; Heneka et al., 2015). In particular, the abnormal activation and dysfunction of microglia can be observed since early disease stages in response to amyloid-beta (Aβ) accumulation (Bolmont et al., 2008; Hanzel et al., 2014). Together with neuronal hypertrophy (Iacono et al., 2008; O'Brien et al., 2009; Oh et al., 2008), the activation of glial cells is thought to be responsible for increased gray matter volume and reduced cortical mean diffusivity observed in the earliest stages of AD (Fortea et al., 2010; Montal et al., 2018).

Progranulin (PGRN) is a highly conserved secreted glycoprotein encoded by the *GRN* gene that is closely associated with microglial function (Pereson et al., 2009). An association between the TT genotype of *GRN* rs5848 single nucleotide polymorphism and the risk of developing late-onset AD has recently been established (Sheng et al., 2014). However, the exact role of PGRN in the pathogenesis of AD is still unclear. It has been suggested that its upregulation may have a beneficial effect on AD pathology by inhibiting and reducing Aβ deposition, whereas PGRN deficiency seems to correlate with increased rates of amyloid and tau accumulation (Hosokawa et al., 2015; Minami et al., 2014). In a recent paper, increasing CSF PGRN levels were observed across different AD stages and correlated with CSF levels of the microglial-derived protein sTREM2. These findings provide support to CSF PGRN as a marker of microglial activation (Suárez-Calvet et al., 2018).

Previous studies have assessed the association between CSF markers of microglial activation, such as sTREM2 and PGRN, with structural measures of neuroinflammation (Araque Caballero et al., 2018; Falcon et al., 2019; Gispert et al., 2016; Morenas-Rodríguez et al., 2016; Suárez-Calvet et al., 2018). In particular, Gispert et al., 2016 described a positive correlation between CSF sTREM2 concentrations with gray matter volume and a negative correlation with mean diffusivity in several brain regions in mild cognitive impairment (MCI) patients. In a following study, the same group showed a

* Corresponding author at: Division of Clinical Geriatrics, Deparment of Neurobiology, Care Sciences and Society, Neo 7th Floor, Blickagången 16, 141 83 Huddinge, Sweden. Tel.: +393280563078; fax: 08-31 11 01.
E-mail address: luciabatzu@gmail.com (L. Batzu).

[1] Data used in preparation of this article were obtained from the Alzheimer's Disease Neuroimaging Initiative (ADNI) database (adni.loni.usc.edu). As such, the investigators within the ADNI contributed to the design and implementation of ADNI and/or provided data but did not participate in analysis or writing of this report. A complete listing of ADNI investigators can be found at: http://adni.loni.usc.edu/wp-content/uploads/how_to_apply/ADNI_Acknowledgement_List.pdf.

0197-4580/$ – see front matter © 2019 Elsevier Inc. All rights reserved.
https://doi.org/10.1016/j.neurobiolaging.2019.12.012

longitudinal association of sTREM2 with gray and white matter volume changes and with mean diffusivity in a cohort of cognitively unimpaired subjects (Falcon et al., 2019). CSF sTREM2 has also been found to correlate with increased global and regional white matter mean diffusivity in a cohort of healthy subjects and AD autosomal dominant mutation carriers. (Araque Caballero et al., 2018). To our knowledge, only two studies have assessed whether CSF PGRN levels are associated with structural neuroimaging measures in AD, but no significant correlations were reported (Morenas-Rodríguez et al., 2016; Suárez-Calvet et al., 2018). However, these studies did not focus on the relationship between PGRN and neuroanatomical measures in the preclinical stages of AD, where neuroinflammatory changes are likely to play an important role in disease pathophysiology (Eikelenboom et al., 2011). Thus, the aim of our study was to assess whether CSF PGRN levels are associated with structural neuroimaging measures, such as cortical thickness (CTh) and subcortical gray matter volumes, in the early phases of the Alzheimer's continuum, and whether this correlation can add new insights into the mechanisms underlying brain changes observed before the onset of brain atrophy. Moreover, we explored whether baseline CSF PGRN levels are associated with neuroanatomical changes in more advanced disease stages and assessed whether they correlate with longitudinal cognitive decline.

2. Methods

2.1. Subjects

Data used in the preparation of this article were obtained from the Alzheimer's Disease Neuroimaging Initiative (ADNI) database (adni.loni.usc.edu). Led by the principal investigator Michael W. Weiner, MD, the ADNI was launched in 2003 as a public-private partnership. The primary goal of ADNI has been to test whether serial magnetic resonance imaging (MRI), positron emission tomography (PET), other biological markers, and clinical and neuropsychological assessment can be combined to measure the progression of MCI and early AD. In the present study, subjects were included if they fulfilled the following criteria: (1) complete CSF measures of Ab1–42, T-Tau, P-Tau, and PGRN at the baseline visit; (2) a CSF biomarker profile that was either normal (A−/TN−) or belonged to the Alzheimer's continuum (A+/TN−, A+/TN+; Jack et al., 2018); (3) had a baseline 3T MRI that passed quality control before and after preprocessing. This resulted in the inclusion of 273 subjects from ADNI 2 database: 122 cognitively normal subjects (CN), 81 subjects with MCI, and 70 subjects with AD dementia. The main inclusion criteria for CN, MCI, and AD participants are displayed in Supplementary Table 1. For a subsample of this cohort (n = 242), the *GRN* rs5848 genotype was available and included in additional analyses. All subjects were assessed with the Alzheimer's Disease Assessment Scale–cognitive subscale 13 (ADAS-Cog 13) (Mohs et al., 1997), the ADNI memory composite score (ADNI-Mem) (Crane et al., 2012) and the ADNI executive function composite score (ADNI-EF) (Gibbons et al., 2012). Written informed consent was given by all participants (or by authorized representatives) and the study was approved by the ethical committees of all institutions.

2.2. CSF analysis

Lumbar puncture was performed to extract CSF levels of β-amyloid 1–42 ($A\beta_{1-42}$), phosphorylated-tau 181P ($P\text{-}tau_{181P}$), total-tau (T-tau), and PGRN. CSF $A\beta_{1-42}$, $P\text{-}tau_{181P}$, and T-tau levels were analyzed using the fully automated Roche Elecsys immunoassays (Bittner et al., 2016; Lifke et al., 2019). The Elecsys β-amyloid (1–42) CSF immunoassay is currently under development, not commercially available and for investigational use only. Performance of the assay has not yet been formally established for $A\beta_{1-42}$ concentrations <200 pg/mL or >1700 pg/mL. None of the subjects of this study had $A\beta_{1-42}$ concentrations <200 pg/mL. Concentrations of $A\beta_{1-42}$ >1700 pg/mL were extrapolated based on a calibration curve. These values are restricted to research purposes and are excluded for clinical decision-making. CSF PGRN was measured by an ELISA protocol performed using a Meso Scale Discovery QuickPlex SQ 120 (Suárez-Calvet et al., 2018).

2.3. Classification of participants

CN subjects were classified into groups with positive (+, abnormal) or negative (−, normal) A/T/(N) biomarkers (Jack et al., 2018) using previously established cutoffs for Elecsys immunoassays ($A\beta_{1-42}$ = 976,6 pg/mL, $P\text{-}tau_{181p}$ = 21,8 pg/mL and T-tau = 245 pg/mL) (Hansson et al., 2018). Owing to the small number of subjects with discrepant T and N classifications (only 5.8%), we merged the T and the N groups, similarly to a previous study (Suárez-Calvet et al., 2018). Because there is strong evidence showing that amyloid pathology is followed by tau accumulation, neurodegeneration, and cognitive impairment in AD, we only included cognitively normal subjects with the following three biomarker profiles: A−/TN−, A+/TN−, A+/TN+ as well as MCI and AD patients who were A+/TN+.

2.4. MRI acquisition and preprocessing

All participants underwent 3T MRI scanning using a T1-weighted Magnetization Prepared RApid Gradient Echo (MPRAGE) sequence with the following parameters: repetition time = 2300–3000 ms; echo time = 3.0–4.1 ms; inversion time = 900 ms; flip angle = 8°; voxel size = 1.1 × 1.1 × 1.2 mm^3. T1-weighted images were preprocessed through our database system (TheHive) (Muehlboeck et al., 2014), using FreeSurfer (version 6.0.0; https://surfer.nmr.mgh.harvard.edu/), as described elsewhere (Pereira et al., 2017).

The CTh maps were smoothed using a full width at half maximum kernel of 15 mm. To perform statistical analyses between subjects, the reconstructed cortical surfaces were registered to the Freesurfer “fsaverage” template using a spherical representation of the cortex. For each subject, the left and right hemispheres were separately inflated to a sphere, which was then deformed to match the curvature map of the analogous sphere in the fsaverage atlas (Fischl et al., 1999). In addition, the volumes of the hippocampus, amygdala, accumbens, pallidum, caudate, putamen, and thalamus, as well as the total intracranial volume, were obtained.

All MRI scans were visually inspected and manual corrections were performed in 6 subjects to fix gray/white-matter surface errors using the Freeview application included in FreeSurfer and according to the protocols described on the software website. In brief, to correct white matter segmentation defects on the reconstructed images, control points were selected where intensity normalization errors were displayed. Failures in the reconstruction of the pial surface due to incorporation of dura mater within the cortical boundaries were fixed after manually deleting voxels belonging to the dura.

2.5. White matter hyperintensities

We also performed additional analyses using the white matter hyperintensity (WMH) volumes computed by the ADNI core laboratory in accordance with previously published protocols (DeCarli et al., 2005).

3. Statistical analysis

3.1. Demographic, cognitive, and CSF variables

Differences between groups in age and sex were assessed using an analysis of variance or χ^2 tests, respectively, in SPSS 25.0 (IBM Corp., Armonk, NY, USA). To assess whether CSF and cognitive variables showed differences between groups, we used an analysis of covariance, while controlling for age and sex (all analyses) in addition to education (cognitive analyses). The *GRN* rs5848 genotype was also added as an additional covariate in a supplementary analysis to assess whether it influenced CSF PRGN levels. Ten outliers were identified in CSF PGRN levels using Tukey's fences method, which were excluded from all analyses. Group comparisons were adjusted for multiple comparisons using false discovery rate (FDR) corrections ($q < 0.05$).

To assess whether CSF PGRN was associated with baseline cognition (ADAS-Cog 13, MMSE, ADNI-Mem, ADNI-EF), given the non-normal distribution of the cognitive scores, partial Spearman's rank correlation analyses were used, while controlling for age, sex, and education. In addition, we used linear mixed effects models to test whether baseline CSF PGRN levels predicted longitudinal cognitive decline using R (R Foundation for Statistical Computing, Vienna, Austria, r-project.org). These analyses included MMSE, ADAS-Cog 13, ADNI-Mem, and ADNI-EF scores as dependent variables in addition to PGRN, time, age, sex, education, and diagnosis as fixed effects. The models included all main effects, the interaction between PGRN and time, and random effects for intercepts. All analyses with cognitive variables were adjusted for multiple comparisons using FDR ($q < 0.05$).

3.2. Imaging variables

3.2.1. Correlation analyses with CSF PGRN

To assess the relationship between CTh and CSF PGRN levels, a general linear model was estimated at each vertex across the cortical surface using FreeSurfer. In this model, CTh was included as the dependent variable, PGRN as a predictor, and age and sex as nuisance variables. The general linear model produced a vertexwise estimate of the "goodness of fit" of CSF PGRN values to each CTh value, while regressing out the effects of age and sex. The parameter estimate was then tested for its significance with a *t*-test. Three supplementary analyses were also performed including GRN rs5848 genotype, WMH volumes (normalized to total intracranial volume) or scan site as additional covariates. Partial Pearson's correlation analyses were performed to assess the relationship between CSF PGRN and subcortical volumes in each diagnostic group, while controlling for the effects of age, sex, and total intracranial volume. The correlation between CSF PGRN and WMH in the whole sample and in each diagnostic group was assessed using Spearman's rank correlation due to non-normal distribution of the WMH data.

3.2.2. Group comparisons

CTh and subcortical gray matter measures were compared between groups. For CTh, general linear models were used within FreeSurfer that included diagnosis as a fixed factor in addition to age and sex as covariates. For subcortical gray matter measures, an analysis of covariance was performed with diagnosis as a factor, while controlling for age, sex, and total intracranial volume.

The CTh results were corrected for multiple comparisons using a clusterwise correction computed with Monte-Carlo simulations (10.000 iterations, clusterwise *p*-threshold <0.05) in FreeSurfer, whereas the subcortical volume analyses were corrected with FDR ($q < 0.05$).

3.2.3. Mediation analysis

To assess the potential role of CSF PGRN in CTh differences between two groups of interest, we conducted a mediation analysis using ordinary least squares regressions with PROCESS macro for SPSS (Hayes, 2013). In this analysis, group was used as dichotomous independent variable (X), mean cortical thickness from significant surface clusters as dependent variable (Y), CSF PGRN as mediator (M), and age and sex as covariates. The coefficients of the linear regressions performed in the mediation analysis were used to define the direct (c'), indirect (ab), and total (c) effects. The significance of the indirect effect (i.e., mediated effect) was assessed by calculating bias-corrected 95% confidence intervals (CIs) using bootstrapping (5000 resamples).

4. Results

4.1. Characteristics of the sample

The characteristics of the sample are shown in Table 1. In total, 65 CN(A−/TN−), 35 CN(A+/TN−), 22 CN(A+/TN+), 81 MCI(A+/TN+), and 70 AD(A+/TN+) were included. No significant differences were found in age or sex between groups. *GRN* rs5848 genotypes were available for 88.64% of the sample ($n = 242$) and no significant differences were found in TT allele prevalence between any of the groups.

4.2. Group differences in CSF PGRN levels

We found a significant group effect in CSF PGRN levels ($F = 7.3$; $p < 0.001$) (Table 1, Fig. 1). Specifically, CN(A+/TN−) subjects displayed the lowest CSF PGRN values compared with all other groups ($p < 0.001$), whereas AD(A+/TN+) patients had significantly higher CSF PGRN levels than MCI(A+/TN+) ($p = 0.004$) and CN(A−/TN−) ($p = 0.008$). After adding the rs5848 genotype as a covariate, these differences in CSF PGRN remained significant.

4.3. Association between CSF PGRN levels with cortical thickness and subcortical gray matter volumes

We found that increasing PGRN levels in CN(A+/TN−) subjects correlated with cortical thickening in the left inferior parietal and right postcentral regions, which extended to the precuneus and other parietal and occipital areas in both hemispheres, as well as in the right temporal cortex. A significant correlation was also present in the left superior and right middle frontal cortices, in addition to other bilateral neighboring areas. (Fig. 2, Supplementary Table 2). In MCI(A+/TN+) and AD(A+/TN+) patients, there was a positive correlation between CSF PGRN and CTh, but this was limited to the right lingual gyrus and right temporal cortex, respectively (Fig. 2). No significant associations were found in the CN(A−/TN−) and CN(A+/TN+) groups. When assessing all subjects in the Alzheimer's continuum (i.e., A+ subjects), increasing CSF PGRN levels correlated with cortical thickening only in the right precentral area (Supplementary Fig. 1).

After adding the GRN rs5848 genotype as a covariate, the areas of positive correlation between CSF PGRN and CTh in the CN(A+/TN−) group were similar, although less extensive (Supplementary Fig. 2). In the MCI(A+/TN+) group, the area of positive correlation in the right lingual gyrus did not survive corrections for multiple comparisons. However, when we performed a partial correlation analysis between extracted CTh mean values of this region and CSF PGRN, while controlling for age, sex, and rs5848 genotype, a

Table 1
Characteristics of the sample

Diagnosis	CN(A−/TN−) n = 65	CN(A+/TN−) n = 35	CN(A+/TN+) n = 22	MCI(A+/TN+) n = 81	AD(A+/TN+) n = 70	*F* or χ^2 (*p* value)
Age	71.2 (5.4)	73.1 (6.1)	74.5 (5.2)	72.0 (6.7)	73.2 (1.1)	1.3 (0.272)
Sex (m/f)	32/33	16/19	8/14	42/39	36/34	2.0 (0.738)
Rs5848 TT (%)[a]	6.3	10.0	10.0	12.1	14.3	2.2 (0.689)
Education[e,j,k]	16.8 (2.6)	16.8 (2.0)	16.4 (2.3)	16.4 (2.7)	15.2 (2.6)	4.5 (0.001)
CDR[d,e,g,h,i,j,k]	0 (0)	0 (0)	0 (0)	0.5 (0)	0.8 (0.2)	398.8 (<0.001)
MMSE[d,e,g,h,i,j,k]	29.3 (1.1)	29.0 (1.4)	29.0 (1.1)	27.2 (1.9)	22.8 (2.1)	145.5 (<0.001)
ADAS-Cog13[d,e,g,h,i,j,k]	8.4 (4.3)	9.1 (4.8)	9.1 (4.0)	19.7 (7.0)	33.3 (8.1)	152.1 (<0.001)
ADNI-Mem[c,d,e,g,h,i,j,k]	1.275 (0.5)	1.072 (0.67)	0.889 (0.6)	−0.147 (0.6)	−0.981 (0.5)	166.7 (<0.001)
ADNI-EF[c,d,e,g,h,j,k]	1.107 (0.8)	0.787 (0.8)	0.368 (0.5)	0.033 (0.8)	−1.017 (0.9)	57.1 (<0.001)
CSF Aβ[b,c,d,e,j] (pg/mL)	1545.5 (316.0)	708.2 (205.0)	744.5 (148.7)	680.6 (155.7)	589.4 (158.8)	217.2 (<0.001)
CSF T-Tau[c,d,e,f,g,h,i,j] (pg/mL)	180.6 (32.0)	164.9 (40.2)	316.9 (72.1)	385.5 (128.2)	418.3 (152.5)	68.2 (<0.001)
CSF P-Tau[c,d,e,f,g,h,i,j] (pg/mL)	15.9 (2.9)	15.1 (4.0)	31.7 (8.5)	39.1 (14.3)	42.0 (16.0)	70.0 (<0.001)
CSF Progranulin[b,e,f,g,h,k] (pg/mL)	1496.2 (253.9)	1304.3 (265.8)	1538.5 (276.9)	1489.4 (301.7)	1625.1 (330.0)	7.3 (<0.001)

Values in the table represent means followed by standard deviation.
Key: CN, cognitively normal; MCI, mild cognitive impairment; AD, Alzheimer's disease; A, aggregated amyloid-beta (- normal/+ pathological); TN, aggregated tau with or without neurodegeneration (- normal/+ pathological); CDR, clinical dementia rating scale; MMSE, Mini–Mental State Examination; ADAS-Cog 13, Alzheimer's disease Assessment Scale–cognitive subscale 13-item; ADNI-Mem, ADNI memory composite score; ADNI-EF, ADNI executive function composite score; CSF, cerebrospinal fluid; Aβ, amyloid-beta; T-Tau, total tau; P-Tau, phosphorylated tau.
[a] Available for a subsample [63 CN(A−/TN−) (96.9%); 30 CN(A+TN−) (85.7%); 20 CN(A+TN+) (90.9%); 66 MCI(A+TN+) (81.5%); 63 AD(A+TN+) (90%)].
[b] Significant difference between CN(A−/TN−) and CN(A+/TN−) ($p < 0.01$).
[c] Significant difference between CN(A−/TN−) and CN(A+/TN+) ($p < 0.01$).
[d] Significant difference between CN(A−/TN−) and MCI(A+/TN+) ($p < 0.01$).
[e] Significant difference between CN(A−/TN−) and AD(A+/TN+) ($p < 0.01$).
[f] Significant difference between CN(A+/TN−) and CN(A+/TN+) ($p < 0.01$).
[g] Significant difference between CN(A+/TN−) and MCI(A+/TN+) ($p < 0.05$).
[h] Significant difference between CN(A+/TN−) and AD(A+/TN+) ($p < 0.01$).
[i] Significant difference between CN(A+/TN+) and MCI(A+/TN+) ($p < 0.01$).
[j] Significant difference between CN(A+/TN+) and AD(A+/TN+) ($p < 0.01$).
[k] Significant difference between MCI(A+/TN+) and AD(A+/TN+) ($p \leq 0.01$).

positive significant correlation was still observed between CTh and CSF PGRN (partial correlation coefficient $\rho_{(TT,age,sex)} = 0.460$, $p =$ 0,00,015). In the AD(A+/TN+) group, a positive correlation was still observed in the right temporal cortex, whereas additional significant correlations with frontal areas were observed. In the Alzheimer's continuum, the significant correlation in the right precentral area remained unchanged (Supplementary Fig. 1).

The results of the analyses including scan site or WMH as covariates can be found in Supplementary Materials and Supplementary Figs. 3 and 4.

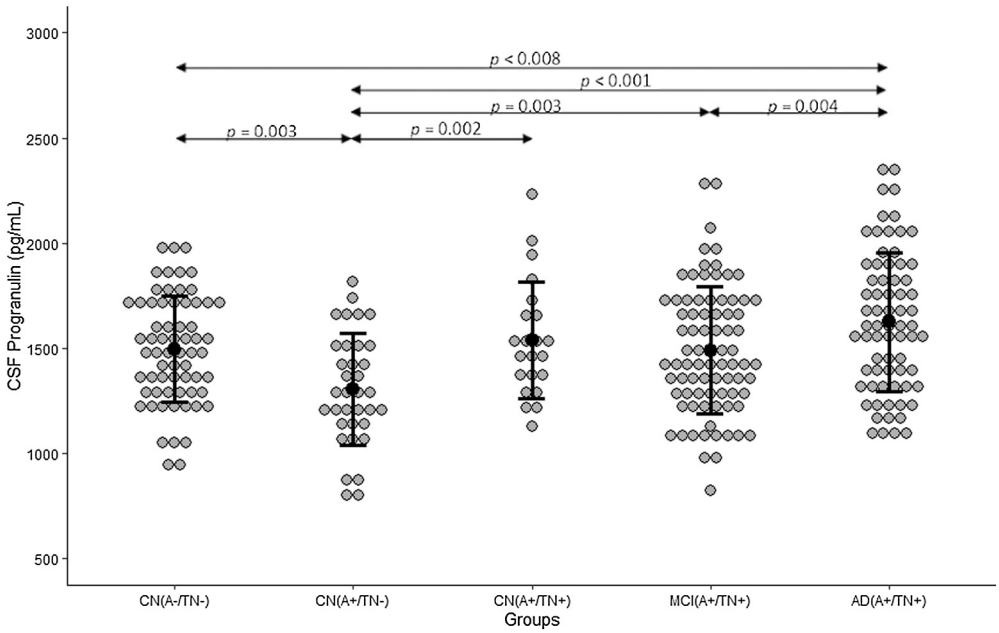

Fig. 1. Differences between groups in CSF progranulin levels. Gray dots represent individual values of CSF progranulin in cognitively normal (CN), mild cognitive impairment (MCI), and Alzheimer's disease (AD) patients with different biomarker profiles. Black dots and bars represent means and standard errors of the mean (SEM), respectively. Key: A, aggregated Aβ; TN, aggregated tau with or without neurodegeneration; −, normal; +, pathological.

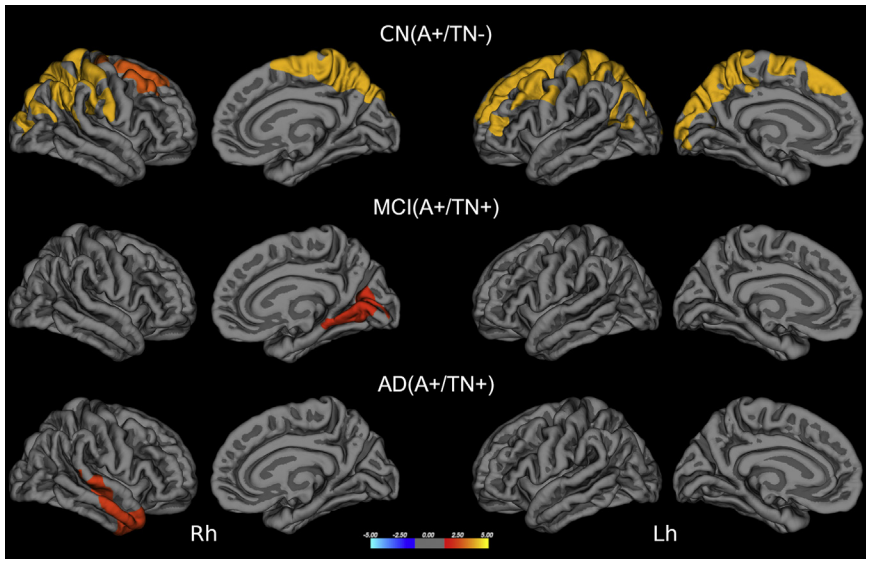

Fig. 2. Correlation between CSF progranulin levels and regional cortical thickness. There were significant correlations between CSF progranulin and cortical thickness in the CN(A+/TN−), MCI(A+/TN+), and AD(A+/TN+) groups after controlling for age and sex ($p < 0.05$; corrected for multiple comparisons). The color scale bar shows the logarithmic scale of p values (−log10). Red-yellow color code means a positive correlation. Key: PGRN, progranulin; CN, cognitively normal; MCI, mild cognitive impairment; AD, Alzheimer's disease; A, aggregated Aβ; TN, aggregated tau with or without neurodegeneration; −, normal; +, pathological; Rh, right hemisphere; Lh, left hemisphere. (For interpretation of the references to color in this figure legend, the reader is referred to the Web version of this article.)

There were no significant correlations between CSF PGRN and subcortical gray matter volumes and between CSF PGRN and WMH volumes.

4.4. Group comparisons of cortical thickness and subcortical gray matter volumes

When comparing CN(A+/TN−) with CN(A−/TN−) subjects, there was increased CTh in the left precuneus, paracentral, postcentral, parietal cortices, and in the right occipital and parietal regions. No regions of decreased CTh were observed in the CN(A+/TN−) group. By contrast, there was cortical thinning in the left middle frontal gyrus in the CN(A+/TN+) group, and in several temporal, parietal, and frontal areas in the MCI(A+/TN+) and AD(A+/TN+) groups (Fig. 3). The analysis of subcortical gray matter volumes did not show differences in CN(A+/TN−) or CN(A+/TN+) compared with CN(A−/TN−). By contrast, MCI(A+/TN+) and AD(A+/TN+) patients showed reduced volumes in the bilateral hippocampus, amygdala, accumbens, and left thalamus, compared with CN(A−/TN−) subjects, in addition to smaller volumes in bilateral putamen in AD(A+/TN−) subjects (Supplementary Table 3).

4.5. The role of PGRN in cortical thickening in early AD

The mediation analysis (Fig. 4) performed to assess the role of CSF PGRN in the cortical thickening observed in CN(A+/TN−) subjects revealed both direct ($c' = 0.978$, $p = 0.001$) and PGRN-mediated ($ab = -0.156$, bootstrap 95% CI from −0.046 to −0.003) effects of groups on CTh. However, these effects were negative, suggesting that PRGN was a suppressor of the cortical thickening observed in CN(A+/TN−) (Fig. 4, Supplementary Table 4).

4.6. CSF PGRN and cognition

There were no significant correlations between CSF PGRN levels and cognition within each group, both at the baseline and longitudinally.

However, when these analyses were carried out across all amyloid-positive subjects (i.e., the Alzheimer's continuum), we found that CSF PGRN levels were associated with worse scores in ADNI-EF ($r_s = -0.212$; $p = 0.001$) at the baseline, similarly to previous findings (Suárez-Calvet et al., 2018) (Supplementary Fig. 5). Moreover, we found that baseline CSF PGRN levels predicted longitudinal decline in global cognition in the Alzheimer's continuum (MMSE and ADAS-Cog 13) ($p = 0.001$), after including diagnosis as an additional covariate (Fig. 5, Supplementary Table 5).

4.7. Assessment of asymmetrical findings

For all analyses where results were observed in only one brain hemisphere, we performed additional analyses to assess whether the other brain hemisphere was also affected or if merging the values from both hemispheres showed similar results. The results of these analyses can be found in Supplementary Material.

5. Discussion

In this study, we observed that CSF levels of PGRN are associated with cortical thickening in the earliest stage of the Alzheimer's continuum, possibly reflecting microglial activation as an early inflammatory event. The areas of cortical thickening observed in early AD stages were partially mediated by PRGN, supporting the hypothesis of “brain swelling” due to neuroinflammation.

5.1. Association between CSF PGRN and cortical thickening as a structural correlate of microglial activation

To our knowledge, this is the first report of a significant correlation between CSF PGRN and structural neuroimaging measures in AD. We observed that higher levels of PGRN in the CSF correlated with higher CTh in bilateral frontoparietal, occipital, and right temporal areas in cognitively normal individuals with amyloid pathology [CN(A+/TN−)]. When performing a separate analysis controlling for *GRN* rs5848 SNP, known to be a modifier of PGRN expression and CSF levels (Morenas-Rodríguez et al., 2016;

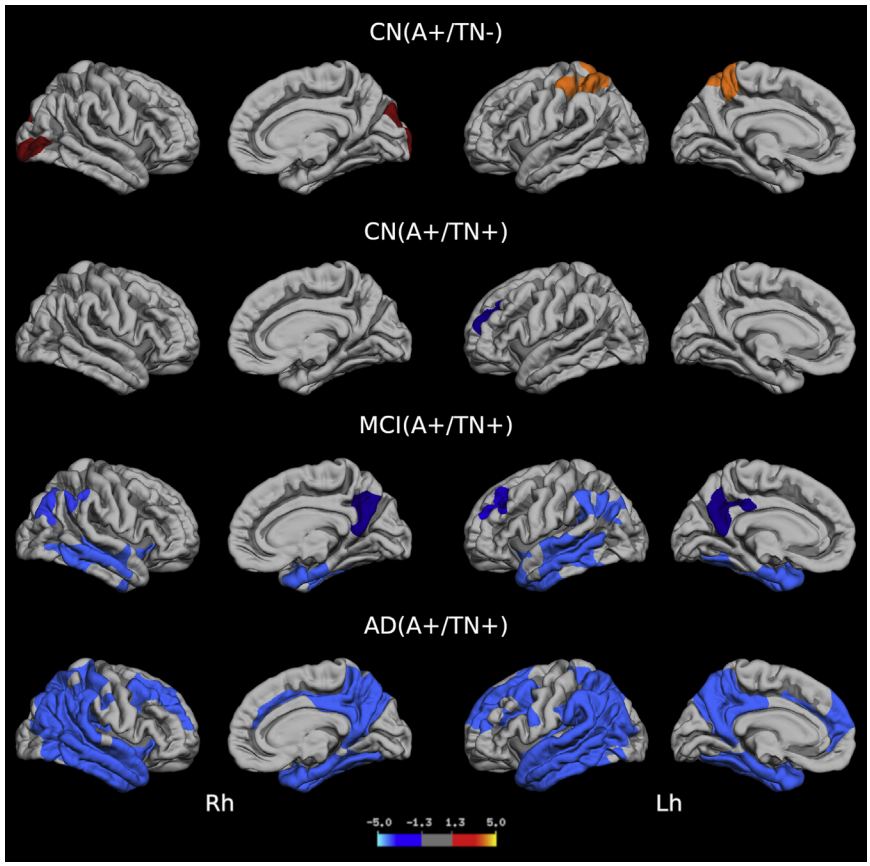

Fig. 3. Differences between groups in cortical thickness. There were significant differences in cortical thickness in all groups compared with the CN(A−/TN−) group ($p < 0.05$; corrected for multiple comparison). The color scale bar shows the logarithmic scale of p values (−log10). Red-yellow color code means increased CTh, and blue color code means decreased CTh. Key: CN, cognitively normal; MCI, mild cognitive impairment; AD, Alzheimer's disease; A, aggregated Aβ; TN, aggregated tau with or without neurodegeneration; −, normal; +, pathological; Rh, right hemisphere; Lh, left hemisphere. (For interpretation of the references to color in this figure legend, the reader is referred to the Web version of this article.)

Nicholson et al., 2014), the correlation was still significant, although less extensive.

In response to neuronal injury, microglial expression of PGRN becomes upregulated (Petkau et al., 2010) to suppress excessive activation, phagocytosis, and production of pro-inflammatory cytokines (Kao et al., 2017; Martens et al., 2012; Yin et al., 2010). In AD, several studies have shown that PGRN expression is highly increased around Aβ plaques, where it acts as microglial chemoattractant and promotes Aβ clearance (Minami et al., 2014; Pereson et al., 2009; Pickford et al., 2011).

Based on these observations, the increased values of CTh related to higher levels of CSF PGRN in CN(A+/TN−) subjects could be interpreted as a macrostructural correlate of microglial recruitment triggered by amyloid pathology.

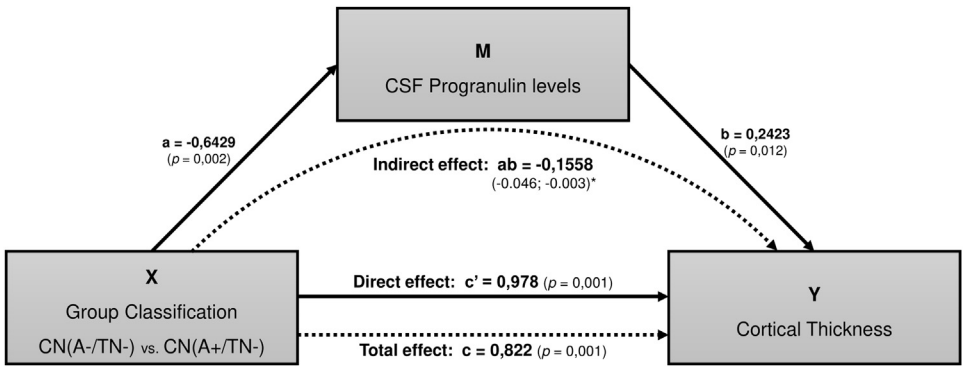

Fig. 4. CSF progranulin is a mediator of cortical thickening changes in early AD stages. Mediation analysis assessing the effects of CSF progranulin in cortical thickness differences between CN(A−/TN−) and CN(A+/TN−) groups: *a*, effect through which group classification (X) influences CSF progranulin levels (M); *b*, effect of M on cortical thickness (Y); *c*, total effect of X on Y, without including M in the model; *c'*, direct effect of X on Y, after adding M to the model; *ab*, influence of X on Y through its effect on M. Partially standardized coefficients and *p* values are reported. Key: CN, cognitively normal; A, aggregated Aβ; TN, aggregated tau with or without neurodegeneration; −, normal; +, pathological. *Significant 95% bootstrap confidence interval (5000 samples).

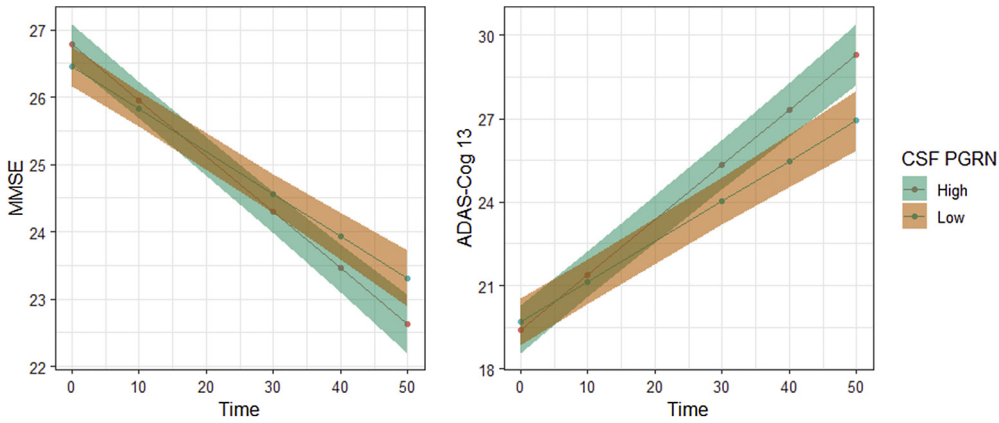

Fig. 5. Significant associations between CSF progranulin and longitudinal cognitive decline. Baseline CSF progranulin values correlated with decline in MMSE ($p < 0.001$) and ADAS-Cog 13 ($p < 0.001$) scores (i.e., lower scores in MMSE and higher scores in ADAS-Cog 13) over time in the Alzheimer's continuum, after correcting for multiple comparisons with FDR ($p < 0.05$). The plots show different trajectories of cognitive decline based on high and low 50th percentiles of CSF PGRN levels. Time is expressed in months from the baseline. Key: PGRN, progranulin; MMSE, Mini–Mental State Examination; ADAS-Cog 13, Alzheimer's disease Assessment Scale–cognitive subscale 13-item.

Interestingly, we did not find any association between CSF PGRN levels and subcortical gray matter structures in the same group. A possible explanation for this lies in the hierarchical involvement of different brain regions in the progression and spreading of Aβ pathology: while the neocortical areas are the first to be affected by amyloid deposition (phase I), the hippocampus, amygdala, and other subcortical structures are involved in later stages of Aβ accumulation (phases II-III) (Thal et al., 2002).

Similarly to previous findings (Suárez-Calvet et al., 2018), we observed higher levels of CSF PGRN in more advanced stages of AD, but only unilateral, positive areas of correlation with CTh were observed in MCI(A+/TN+) and AD(A+/TN+) groups and no associations were found in the CN(A+/TN+) group. We could hypothesize that the augmented PGRN levels reflect a pathological response to increasing amyloid and p-tau pathology as well as an attempt to modulate chronic neuroinflammation and neuronal damage. Microglial activation is considered to be present even in later stages of AD, although shifted toward a proinflammatory phenotype (Fan et al., 2017), hence the existence of areas of positive correlation between CSF PGRN and CTh also in MCI(A+/TN+) and AD(A+/TN+) groups.

5.2. Neuroinflammation and increased cortical thickness in early stages of the Alzheimer's continuum

Our group comparisons showed decreased CTh in CN(A+/TN+), MCI(A+/TN+), and AD(A+/TN−) groups, when compared with the CN(A−/TN−) group, in agreement with previous findings (Dickerson et al., 2009). By contrast, the CN(A+/TN−) group showed increased CTh in the precuneus, lateral parietal, and occipital areas. These findings agree with previous studies showing increased CTh in the bilateral precuneus and other parietal areas in asymptomatic *PSEN1* mutation carriers (Fortea et al., 2010; Sala-Llonch et al., 2015). They also agree with studies showing increased gray matter volumes in Aβ-positive cognitively normal subjects, children carrying *PSEN1* mutations (Johnson et al., 2014; Quiroz et al., 2015) and sporadic preclinical AD cohorts (Chételat et al., 2010; Fortea et al., 2011, 2014; Montal et al., 2018; Pegueroles et al., 2017). Altogether, these observations indicate that increased gray matter in early AD stages could be an early neuroinflammatory response to amyloid deposition. Reactive neuronal hypertrophy, microgliosis, and astrocytosis may be responsible for the areas of cortical thickening we observed in the CN(A+/TN−) group.

Several studies reported neuroimaging and neuropathological evidence of neuronal hypertrophy, gliosis and increased cortical thickness/subcortical gray matter volumes in transgenic AD mouse models, occurring at an early stage of amyloid deposition or even preceding it (Badhwar et al., 2013; Grand'Maison et al., 2013; Hanzel et al., 2014; Maheswaran et al., 2009; Oh et al., 2008). Similar findings were observed in neuropathological studies on asymptomatic AD subjects (Iacono et al., 2008; O'Brien et al., 2009). Results from an Aβ immunotherapy trial have also shown a decrease in whole-brain volume in antibody responders as a possible consequence of Aβ-associated gliosis (Fox et al., 2005). Moreover, CSF levels of sTREM2 were found to be associated with cortical volume increases in patients with MCI (Gispert et al., 2016), and microglial activation, quantified using [^{11}C]PBR28 PET, was associated with higher gray matter volume in patients with MCI (Femminella et al., 2019). Our results can be interpreted in this context: an early and active involvement of PGRN in microglia activation might be associated with detectable structural changes, such as increased CTh, in the initial stages of AD pathology. In fact, although some PGRN-correlated areas, such as the precentral and postcentral gyri, are not among those that display early neocortical amyloid deposition (Grothe et al., 2017), they were previously described to have increased CTh in asymptomatic *PSEN1* mutation carriers compared with controls and interpreted as a result of possible early neuroinflammatory mechanisms (Sala-Llonch et al., 2015). Future studies are needed to elucidate the cause of this discrepancy.

5.3. CSF PGRN correlation with CTh occurs at the lowest CSF PGRN levels

Similarly to a previous study (Suárez-Calvet et al., 2018), when comparing CSF PGRN levels among the different diagnostic groups, we found the lowest levels in the CN(A+/TN−) group. Although it may appear contradictory, this finding could have different explanations. For instance, it has been hypothesized that microglial PGRN expression could be affected by the status of Aβ peptides, being downregulated in the presence of abundant Aβ oligomers and upregulated in the presence of Aβ fibrils associated with plaques (Minami et al., 2014). However, it is now established that low PGRN expression constitutes a risk factor for AD, and the low CSF PGRN levels we observed in Aβ-positive subjects could be a defining feature of a group at higher risk of developing the disease.

5.4. The role of PGRN on early structural brain changes and cognition: beneficial or detrimental?

Whether PGRN has a beneficial or detrimental role in AD pathophysiology is still under debate (Minami et al., 2014; Takahashi et al., 2017). Notwithstanding, we can interpret our findings in the CN(A+/TN−) group from two different perspectives. First, the positive association between CSF PGRN and CTh could suggest a protective effect of PGRN, probably due to the earliest phase of microglial activation, preserving the volume of gray matter despite the presence of amyloid pathology. Second, the observed areas of cortical thickening, when compared with CN(A−/TN−) subjects, could reflect an actual regional "brain swelling" due to neuroinflammation, with uncertain effect on disease progression.

Our results may also be explained in light of increasing evidence showing the presence of different microglial phenotypes in AD (Dubbelaar et al., 2018). In particular, the alteration of a delicate balance between a homeostatic microglial (HM) signature and a microglial neurodegenerative phenotype (MGnD) is thought to be involved in the dysfunctional neuroinflammatory response seen in AD pathophysiology (Götzl et al., 2019). Moreover, it has been shown that TREM2-deficient and PGRN-deficient mice displayed opposite activation states and functional phenotypes of microglia: loss of TREM2 would be responsible for locking microglia in an HM state while loss of PGRN would result in an MGnD phenotype and exaggerated neuroinflammation (Götzl et al., 2019; Krasemann et al., 2017). In this context, the protective role of PGRN in modulating neuroinflammation through the expression of a phenotype more shifted to the HM state in the earliest stage of the Alzheimer's continuum is likely. In the mediation analysis, we found that PGRN had a significant effect on the group differences in CTh. After controlling for the effect of PGRN in the model, the differences between groups became higher, suggesting that PGRN at least partially suppressed the "brain swelling" observed in CN(A+/TN−) compared with CN(A−/TN−). These results support the protective role of PGRN on brain structure during early AD-related neuroinflammation.

However, the areas that showed cortical thinning in the MCI and AD groups only partially overlapped with the areas where CTh correlated with increased CSF PGRN in the CN(A+/TN−) group (e.g., precuneus, inferior parietal and superior frontal cortices). This suggests that PGRN may not be involved in the specific pattern of brain atrophy observed in more advanced stages of AD.

Regarding the relationship between CSF PGRN and clinical features, in a recent study (Suárez-Calvet et al., 2018), increased CSF PGRN levels were found to be associated with worse cognition in subjects in the Alzheimer's continuum. In our sample, although similar results were obtained, the correlations in the separate groups did not show significant results. This, together with the absence of differences in cognitive performance between CN(A+/TN−) and CN(A−/TN−) subjects, suggests that the observed structural features related to CSF PGRN levels in the CN(A+/TN−) group may not have a clinical correlate. However, in the Alzheimer's continuum, higher CSF PGRN levels at the baseline predicted a worse decline in overall cognition (MMSE and ADAS-Cog 13) at follow-up, suggesting that the abnormally increased levels associated with AD pathology may have a detrimental effect on cognitive decline.

5.5. Limitations

Our study has several limitations. First, some of the groups were relatively small, which may have limited our ability to detect cognitive associations with PGRN within each group. Second, microglial activation in our sample was not directly assessed using PET imaging and the assumption that the observed structural correlation between CTh and CSF PGRN levels is due to microglial activation is based on previous evidence of microglia as the major responsible for PGRN expression (Yin et al., 2010). Moreover, we could not reproduce our results using CSF Aβ42/Aβ40 ratios instead of CSF Aβ42 levels as a biomarker for amyloid pathology. There is increasing evidence that this ratio could provide more accurate information about the status of amyloid pathology in the brain, as it may correct for interindividual variability in the overall Aβ production (Janelidze et al., 2016). Unfortunately, the Aβ40 levels have been measured with the Elecsys immunoassay only in ADNI 3 subjects so we could not use them in the present study to confirm that the low levels of CSF PGRN observed in the earliest stage of the disease are truly given by an Aβ-related downregulation.

6. Conclusions

Our findings add new insights to the relationship between progranulin and AD. By showing that PGRN is associated with cortical thickening in early AD and that it partially mediates the brain swelling observed in the first disease stage, we provide support to the role of progranulin as an early biomarker of anatomical neuroinflammation. Further research is needed to confirm whether the active involvement of progranulin is limited to the earliest phases of AD, after which its increase could be no longer beneficial, offering a potential window to implement therapeutic strategies involving progranulin administration.

Disclosure Statement

The authors have no potential financial or personal conflicts of interest.

Acknowledgements

Data collection and sharing for this project was funded by the Alzheimer's Disease Neuroimaging Initiative (National Institutes of Health Grant U01 AG024904) and DOD ADNI (Department of Defense award number W81XWH-12-2-0012). ADNI is funded by the National Institute on Aging, the National Institute of Biomedical Imaging and Bioengineering, and through generous contributions from the following: AbbVie, Alzheimer's Association; Alzheimer's Drug Discovery Foundation; Araclon Biotech; BioClinica, Inc.; Biogen; Bristol-Myers Squibb Company; CereSpir, Inc.; Cogstate; Eisai Inc.; Elan Pharmaceuticals, Inc.; Eli Lilly and Company; EuroImmun; F. Hoffmann-La Roche Ltd and its affiliated company Genentech, Inc.; Fujirebio; GE Healthcare; IXICO Ltd.; Janssen Alzheimer Immunotherapy Research & Development, LLC.; Johnson & Johnson Pharmaceutical Research & Development LLC.; Lumosity; Lundbeck; Merck & Co., Inc.; Meso Scale Diagnostics, LLC.; NeuroRx Research; Neurotrack Technologies; Novartis Pharmaceuticals Corporation; Pfizer Inc.; Piramal Imaging; Servier; Takeda Pharmaceutical Company; and Transition Therapeutics. The Canadian Institutes of Health Research is providing funds to support ADNI clinical sites in Canada. Private sector contributions are facilitated by the Foundation for the National Institutes of Health (www.fnih.org). The grantee organization is the Northern California Institute for Research and Education, and the study is coordinated by the Alzheimer's Therapeutic Research Institute at the University of Southern California. ADNI data are disseminated by the Laboratory for Neuro Imaging at the University of Southern California.

The author's research groups were supported by the Swedish Research Council, Alzheimerfonden, Hjärnfonden, the Strategic Research Programme in Neuroscience at Karolinska Institutet (StratNeuro), the Swedish Foundation for Strategic Research (SSF)

and Birgitta och Sten Westerberg. The funding sources had no role in the design and conduct of the study; in the collection, analysis, interpretation of the data; or in the preparation, review, or approval of the manuscript.

Author Contribution Statement: Lucia Batzu: Conceptualization, Methodology, Formal analysis, Investigation, Writing - original draft; Eric Westman: Writing - review & editing; Joana B. Pereira: Conceptualization, Methodology, Writing - review & editing; Supervision.

Appendix A. Supplementary data

Supplementary data associated with this article can be found, in the online version, at https://doi.org/10.1016/j.neurobiolaging.2019.12.012.

References

Araque Caballero, M.A., Suárez-Calvet, M., Duering, M., Franzmeier, N., Benzinger, T., Fagan, A.M., Bateman, R.J., Jack, C.R., Levin, J., Dichgans, M., Jucker, M., Karch, C., Masters, C.L., Morris, J.C., Weiner, M., Rossor, M., Fox, N.C., Lee, J.-H., Salloway, S., Danek, A., Goate, A., Yakushev, I., Hassenstab, J., Schofield, P.R., Haass, C., Ewers, M., 2018. White matter diffusion alterations precede symptom onset in autosomal dominant Alzheimer's disease. Brain 141, 3065–3080.

Badhwar, A., Lerch, J.P., Hamel, E., Sled, J.G., 2013. Impaired structural correlates of memory in Alzheimer's disease mice. Neuroimage Clin. 3, 290–300.

Bittner, T., Zetterberg, H., Teunissen, C.E., Ostlund, R.E., Militello, M., Andreasson, U., Hubeek, I., Gibson, D., Chu, D.C., Eichenlaub, U., Heiss, P., Kobold, U., Leinenbach, A., Madin, K., Manuilova, E., Rabe, C., Blennow, K., 2016. Technical performance of a novel, fully automated electrochemiluminescence immunoassay for the quantitation of β-amyloid (1–42) in human cerebrospinal fluid. Alzheimers Dement. 12, 517–526.

Bolmont, T., Haiss, F., Eicke, D., Radde, R., Mathis, C.A., Klunk, W.E., Kohsaka, S., Jucker, M., Calhoun, M.E., 2008. Dynamics of the microglial/amyloid interaction indicate a role in plaque maintenance. J. Neurosci. 28, 4283–4292.

Chételat, G., Villemagne, V.L., Pike, K.E., Baron, J.-C., Bourgeat, P., Jones, G., Faux, N.G., Ellis, K.A., Salvado, O., Szoeke, C., Martins, R.N., Ames, D., Masters, C.L., Rowe, C.C., 2010. Larger temporal volume in elderly with high versus low beta-amyloid deposition. Brain 133, 3349–3358.

Crane, P.K., Carle, A., Gibbons, L.E., Insel, P., Mackin, R.S., Gross, A., Jones, R.N., Mukherjee, S., Curtis, S.M., Harvey, D., Weiner, M., Mungas, D., 2012. Development and assessment of a composite score for memory in the Alzheimer's Disease Neuroimaging Initiative (ADNI). Brain Imaging Behav. 6, 502–516.

DeCarli, C., Fletcher, E., Ramey, V., Harvey, D., Jagust, W.J., 2005. Anatomical mapping of white matter hyperintensities (WMH): exploring the relationships between periventricular WMH, deep WMH, and total WMH burden. Stroke 36, 50–55.

Dickerson, B.C., Bakkour, A., Salat, D.H., Feczko, E., Pacheco, J., Greve, D.N., Grodstein, F., Wright, C.I., Blacker, D., Rosas, H.D., Sperling, R.A., Atri, A., Growdon, J.H., Hyman, B.T., Morris, J.C., Fischl, B., Buckner, R.L., 2009. The cortical signature of Alzheimer's disease: regionally specific cortical thinning relates to symptom severity in very mild to mild AD dementia and is detectable in asymptomatic amyloid-positive individuals. Cereb. Cortex 19, 497–510.

Dubbelaar, M.L., Kracht, L., Eggen, B.J.L., Boddeke, E.W.G.M., 2018. The kaleidoscope of microglial phenotypes. Front. Immunol. 9, 1753.

Eikelenboom, P., Veerhuis, R., van Exel, E., Hoozemans, J.J.M., Rozemuller, A.J.M., van Gool, W.A., 2011. The early involvement of the innate immunity in the pathogenesis of late-onset Alzheimer's disease. Neuropathological, epidemiological and genetic evidence. Curr. Alzheimer Res. 8, 142–150.

Falcon, C., Monté-Rubio, G.C., Grau-Rivera, O., Suárez-Calvet, M., Sánchez-Valle, R., Rami, L., Bosch, B., Haass, C., Gispert, J.D., Molinuevo, J.L., 2019. CSF glial biomarkers YKL40 and sTREM2 are associated with longitudinal volume and diffusivity changes in cognitively unimpaired individuals. Neuroimage Clin. 23, 101801.

Fan, Z., Brooks, D.J., Okello, A., Edison, P., 2017. An early and late peak in microglial activation in Alzheimer's disease trajectory. Brain 140, 792–803.

Femminella, G.D., Dani, M., Wood, M., Fan, Z., Calsolaro, V., Atkinson, R., Edginton, T., Hinz, R., Brooks, D.J., Edison, P., 2019. Microglial activation in early Alzheimer trajectory is associated with higher gray matter volume. Neurology 92, e1331–e1343.

Fischl, B., Sereno, M.I., Tootell, R.B., Dale, A.M., 1999. High-resolution intersubject averaging and a coordinate system for the cortical surface. Hum. Brain Mapp. 8, 272–284.

Fortea, J., Sala-Llonch, R., Bartrés-Faz, D., Bosch, B., Lladó, A., Bargalló, N., Molinuevo, J.L., Sánchez-Valle, R., 2010. Increased cortical thickness and caudate volume precede atrophy in PSEN1 mutation carriers. J. Alzheimers Dis. 22, 909–922.

Fortea, J., Sala-Llonch, R., Bartrés-Faz, D., Lladó, A., Solé-Padullés, C., Bosch, B., Antonell, A., Olives, J., Sanchez-Valle, R., Molinuevo, J.L., Rami, L., 2011. Cognitively preserved subjects with transitional cerebrospinal fluid ß-amyloid 1-42 values have thicker cortex in Alzheimer's disease vulnerable areas. Biol. Psychiatry 70, 183–190.

Fortea, J., Vilaplana, E., Alcolea, D., Carmona-Iragui, M., Sánchez-Saudinos, M.-B., Sala, I., Antón-Aguirre, S., González, S., Medrano, S., Pegueroles, J., Morenas, E., Clarimón, J., Blesa, R., Lleó, A., 2014. Cerebrospinal fluid β-amyloid and phospho-tau biomarker interactions affecting brain structure in preclinical Alzheimer disease. Ann. Neurol. 76, 223–230.

Fox, N.C., Black, R.S., Gilman, S., Rossor, M.N., Griffith, S.G., Jenkins, L., Koller, M., 2005. Effects of Aβ immunization (AN1792) on MRI measures of cerebral volume in Alzheimer disease. Neurology 64, 1563–1572.

Gibbons, L.E., Carle, A.C., Mackin, R.S., Harvey, D., Mukherjee, S., Insel, P., Curtis, S.M., Mungas, D., Crane, P.K., 2012. A composite score for executive functioning, validated in Alzheimer's Disease Neuroimaging Initiative (ADNI) participants with baseline mild cognitive impairment. Brain Imaging Behav. 6, 517–527.

Gispert, J.D., Suárez-Calvet, M., Monté, G.C., Tucholka, A., Falcon, C., Rojas, S., Rami, L., Sánchez-Valle, R., Lladó, A., Kleinberger, G., Haass, C., Molinuevo, J.L., 2016. Cerebrospinal fluid sTREM2 levels are associated with gray matter volume increases and reduced diffusivity in early Alzheimer's disease. Alzheimers Dement. 12, 1259–1272.

Götzl, J.K., Brendel, M., Werner, G., Parhizkar, S., Sebastian Monasor, L., Kleinberger, G., Colombo, A., Deussing, M., Wagner, M., Winkelmann, J., Diehl-Schmid, J., Levin, J., Fellerer, K., Reifschneider, A., Bultmann, S., Bartenstein, P., Rominger, A., Tahirovic, S., Smith, S.T., Madore, C., Butovsky, O., Capell, A., Haass, C., 2019. Opposite microglial activation stages upon loss of PGRN or TREM2 result in reduced cerebral glucose metabolism. EMBO Mol. Med. 11, e9711.

Grand'Maison, M., Zehntner, S.P., Ho, M.-K., Hébert, F., Wood, A., Carbonell, F., Zijdenbos, A.P., Hamel, E., Bedell, B.J., 2013. Early cortical thickness changes predict β-amyloid deposition in a mouse model of Alzheimer's disease. Neurobiol. Dis. 54, 59–67.

Grothe, M.J., Barthel, H., Sepulcre, J., Dyrba, M., Sabri, O., Teipel, S.J., 2017. In vivo staging of regional amyloid deposition. Neurology 89, 2031–2038.

Hansson, O., Seibyl, J., Stomrud, E., Zetterberg, H., Trojanowski, J.Q., Bittner, T., Lifke, V., Corradini, V., Eichenlaub, U., Batrla, R., Buck, K., Zink, K., Rabe, C., Blennow, K., Shaw, L.M., 2018. CSF biomarkers of Alzheimer's disease concord with amyloid-β PET and predict clinical progression: a study of fully automated immunoassays in BioFINDER and ADNI cohorts. Alzheimers Dement. 14, 1470–1481.

Hanzel, C.E., Pichet-Binette, A., Pimentel, L.S.B., Iulita, M.F., Allard, S., Ducatenzeiler, A., Do Carmo, S., Cuello, A.C., 2014. Neuronal driven pre-plaque inflammation in a transgenic rat model of Alzheimer's disease. Neurobiol. Aging 35, 2249–2262.

Hayes, A.F., 2013. Introduction to Mediation, Moderation, and Conditional Process Analysis: A Regression-Based Approach. Guilford Press, New York.

Heneka, M.T., Carson, M.J., Khoury, J.E., Landreth, G.E., Brosseron, F., Feinstein, D.L., Jacobs, A.H., Wyss-Coray, T., Vitorica, J., Ransohoff, R.M., Herrup, K., Frautschy, S.A., Finsen, B., Brown, G.C., Verkhratsky, A., Yamanaka, K., Koistinaho, J., Latz, E., Halle, A., Petzold, G.C., Town, T., Morgan, D., Shinohara, M.L., Perry, V.H., Holmes, C., Bazan, N.G., Brooks, D.J., Hunot, S., Joseph, B., Deigendesch, N., Garaschuk, O., Boddeke, E., Dinarello, C.A., Breitner, J.C., Cole, G.M., Golenbock, D.T., Kummer, M.P., 2015. Neuroinflammation in Alzheimer's disease. Lancet Neurol. 14, 388–405.

Hosokawa, M., Arai, T., Masuda-Suzukake, M., Kondo, H., Matsuwaki, T., Nishihara, M., Hasegawa, M., Akiyama, H., 2015. Progranulin reduction is associated with increased tau phosphorylation in P301L tau transgenic mice. J. Neuropathol. Exp. Neurol. 74, 158–165.

Iacono, D., O'Brien, R., Resnick, S.M., Zonderman, A.B., Pletnikova, O., Rudow, G., An, Y., West, M.J., Crain, B., Troncoso, J.C., 2008. Neuronal hypertrophy in asymptomatic Alzheimer disease. J. Neuropathol. Exp. Neurol. 67, 578–589.

Jack, C.R., Bennett, D.A., Blennow, K., Carrillo, M.C., Dunn, B., Haeberlein, S.B., Holtzman, D.M., Jagust, W., Jessen, F., Karlawish, J., Liu, E., Molinuevo, J.L., Montine, T., Phelps, C., Rankin, K.P., Rowe, C.C., Scheltens, P., Siemers, E., Snyder, H.M., Sperling, R., Elliott, C., Masliah, E., Ryan, L., Silverberg, N., 2018. NIA-AA Research Framework: toward a biological definition of Alzheimer's disease. Alzheimers Dement. 14, 535–562.

Janelidze, S., Zetterberg, H., Mattsson, N., Palmqvist, S., Vanderstichele, H., Lindberg, O., van Westen, D., Stomrud, E., Minthon, L., Blennow, K., Hansson, O., 2016. CSF Abeta42/Abeta40 and Abeta42/Abeta38 ratios: better diagnostic markers of Alzheimer disease. Ann. Clin. Transl. Neurol. 3, 154–165.

Johnson, S.C., Christian, B.T., Okonkwo, O.C., Oh, J.M., Harding, S., Xu, G., Hillmer, A.T., Wooten, D.W., Murali, D., Barnhart, T.E., Hall, L.T., Racine, A.M., Klunk, W.E., Mathis, C.A., Bendlin, B.B., Gallagher, C.L., Carlsson, C.M., Rowley, H.A., Hermann, B.P., Dowling, N.M., Asthana, S., Sager, M.A., 2014. Amyloid burden and neural function in people at risk for Alzheimer's Disease. Neurobiol. Aging 35, 576–584.

Kao, A.W., McKay, A., Singh, P.P., Brunet, A., Huang, E.J., 2017. Progranulin, lysosomal regulation and neurodegenerative disease. Nat. Rev. Neurosci. 18, 325–333.

Krasemann, S., Madore, C., Cialic, R., Baufeld, C., Calcagno, N., El Fatimy, R., Beckers, L., O'Loughlin, E., Xu, Y., Fanek, Z., Greco, D.J., Smith, S.T., Tweet, G., Humulock, Z., Zrzavy, T., Conde-Sanroman, P., Gacias, M., Weng, Z., Chen, H., Tjon, E., Mazaheri, F., Hartmann, K., Madi, A., Ulrich, J.D., Glatzel, M., Worthmann, A., Heeren, J., Budnik, B., Lemere, C., Ikezu, T., Heppner, F.L., Litvak, V., Holtzman, D.M., Lassmann, H., Weiner, H.L., Ochando, J., Haass, C., Butovsky, O., 2017. The TREM2-APOE pathway drives the transcriptional

phenotype of dysfunctional microglia in neurodegenerative diseases. Immunity 47, 566–581.
Lifke, V., Kollmorgen, G., Manuilova, E., Oelschlaegel, T., Hillringhaus, L., Widmann, M., von Arnim, C.A.F., Otto, M., Christenson, R.H., Powers, J.L., Shaw, L.M., Hansson, O., Doecke, J.D., Li, Q.-X., Teunissen, C., Tumani, H., Blennow, K., 2019. Elecsys® Total-Tau and Phospho-Tau (181P) CSF assays: analytical performance of the novel, fully automated immunoassays for quantification of tau proteins in human cerebrospinal fluid. Clin. Biochem. 72, 30–38.
Maheswaran, S., Barjat, H., Rueckert, D., Bate, S.T., Howlett, D.R., Tilling, L., Smart, S.C., Pohlmann, A., Richardson, J.C., Hartkens, T., Hill, D.L.G., Upton, N., Hajnal, J.V., James, M.F., 2009. Longitudinal regional brain volume changes quantified in normal aging and Alzheimer's APP×PS1 mice using MRI. Brain Res. 1270, 19–32.
Martens, L.H., Zhang, J., Barmada, S.J., Zhou, P., Kamiya, S., Sun, B., Min, S.-W., Gan, L., Finkbeiner, S., Huang, E.J., Farese, R.V., 2012. Progranulin deficiency promotes neuroinflammation and neuron loss following toxin-induced injury. J. Clin. Invest. 122, 3955–3959.
Minami, S.S., Min, S.-W., Krabbe, G., Wang, C., Zhou, Y., Asgarov, R., Li, Y., Martens, L.H., Elia, L.P., Ward, M.E., Mucke, L., Farese, R.V., Gan, L., 2014. Progranulin protects against amyloid β deposition and toxicity in Alzheimer's disease mouse models. Nat. Med. 20, 1157–1164.
Mohs, R.C., Knopman, D., Petersen, R.C., Ferris, S.H., Ernesto, C., Grundman, M., Sano, M., Bieliauskas, L., Geldmacher, D., Clark, C., Thal, L.J., 1997. Development of cognitive instruments for use in clinical trials of antidementia drugs: additions to the Alzheimer's Disease Assessment Scale that broaden its scope. The Alzheimer's Disease Cooperative Study. Alzheimer Dis. Assoc. Disord. 11 (Suppl. 2), S13–S21.
Montal, V., Vilaplana, E., Alcolea, D., Pegueroles, J., Pasternak, O., González-Ortiz, S., Clarimón, J., Carmona-Iragui, M., Illán-Gala, I., Morenas-Rodríguez, E., Ribosa-Nogué, R., Sala, I., Sánchez-Saudinós, M.B., García-Sebastian, M., Villanúa, J., Izagirre, A., Estanga, A., Ecay-Torres, M., Iriondo, A., Clerigue, M., Tainta, M., PozuetaA, A., González, A., Martínez-Heras, E., Llufriu, S., Blesa, R., Sanchez-Juan, P., Martínez-Lage, P., Lleó, A., Fortea, J., 2018. Cortical microstructural changes along the Alzheimer's disease continuum. Alzheimers Dement. 14, 340–351.
Morenas-Rodríguez, E., Cervera-Carles, L., Vilaplana, E., Alcolea, D., Carmona-Iragui, M., Dols-Icardo, O., Ribosa-Nogué, R., Muñoz-Llahuna, L., Sala, I., Belén Sánchez-Saudinós, M., Blesa, R., Clarimón, J., Fortea, J., Lleó, A., 2016. Progranulin protein levels in cerebrospinal fluid in primary neurodegenerative dementias. J. Alzheimers Dis. 50, 539–546.
Muehlboeck, J.-S., Westman, E., Simmons, A., 2014. TheHiveDB image data management and analysis framework. Front. Neuroinform. 7, P389.
Nicholson, A.M., Finch, N.A., Thomas, C.S., Wojtas, A., Rutherford, N.J., Mielke, M.M., Roberts, R.O., Boeve, B.F., Knopman, D.S., Petersen, R.C., Rademakers, R., 2014. Progranulin protein levels are differently regulated in plasma and CSF. Neurology 82, 1871–1878.
O'Brien, R.J., Resnick, S.M., Zonderman, A.B., Ferrucci, L., Crain, B.J., Pletnikova, O., Rudow, G., Iacono, D., Riudavets, M.A., Driscoll, I., Price, D.L., Martin, L.J., Troncoso, J.C., 2009. Neuropathologic studies of the Baltimore longitudinal study of aging (BLSA). J. Alzheimers Dis. 18, 665–675.
Oh, E.S., Savonenko, A.V., King, J.F., Fangmark Tucker, S.M., Rudow, G.L., Xu, G., Borchelt, D.R., Troncoso, J.C., 2008. Amyloid precursor protein increases cortical neuron size in transgenic mice. Neurobiol. Aging 30, 1238–1244.
Pegueroles, J., Vilaplana, E., Montal, V., Sampedro, F., Alcolea, D., Carmona-Iragui, M., Clarimon, J., Blesa, R., Lleó, A., Fortea, J., 2017. Longitudinal brain structural changes in preclinical Alzheimer's disease. Alzheimers Dement. 13, 499–509.
Pereira, J.B., Westman, E., Hansson, O., 2017. Association between cerebrospinal fluid and plasma neurodegeneration biomarkers with brain atrophy in Alzheimer's disease. Neurobiol. Aging 58, 14–29.
Pereson, S., Wils, H., Kleinberger, G., McGowan, E., Vandewoestyne, M., Van Broeck, B., Joris, G., Cuijt, I., Deforce, D., Hutton, M., Van Broeckhoven, C., Kumar-Singh, S., 2009. Progranulin expression correlates with dense-core amyloid plaque burden in Alzheimer disease mouse models. J. Pathol. 219, 173–181.
Petkau, T.L., Neal, S.J., Orban, P.C., MacDonald, J.L., Hill, A.M., Lu, G., Feldman, H.H., MacKenzie, I.R.A., Leavitt, B.R., 2010. Progranulin expression in the developing and adult murine brain. J. Comp. Neurol. 518, 3931–3947.
Pickford, F., Marcus, J., Camargo, L.M., Xiao, Q., Graham, D., Mo, J.-R., Burkhardt, M., Kulkarni, V., Crispino, J., Hering, H., Hutton, M., 2011. Progranulin is a chemoattractant for microglia and stimulates their Endocytic activity. Am. J. Pathol. 178, 284–295.
Quiroz, Y.T., Schultz, A.P., Chen, K., Protas, H.D., Brickhouse, M., Fleisher, A.S., Langbaum, J.B., Thiyyagura, P., Fagan, A.M., Shah, A.R., Muniz, M., Arboleda-Velasquez, J.F., Munoz, C., Garcia, G., Acosta-Baena, N., Giraldo, M., Tirado, V., Ramírez, D.L., Tariot, P.N., Dickerson, B.C., Sperling, R.A., Lopera, F., Reiman, E.M., 2015. Brain imaging and blood biomarker abnormalities in children with autosomal dominant alzheimer disease. JAMA Neurol. 72, 912.
Sala-Llonch, R., Lladó, A., Fortea, J., Bosch, B., Antonell, A., Balasa, M., Bargalló, N., Bartrés-Faz, D., Molinuevo, J.L., Sánchez-Valle, R., 2015. Evolving brain structural changes in PSEN1 mutation carriers. Neurobiol. Aging 36, 1261–1270.
Sheng, J., Su, L., Xu, Z., Chen, G., 2014. Progranulin polymorphism rs5848 is associated with increased risk of Alzheimer's disease. Gene 542, 141–145.
Suárez-Calvet, M., Capell, A., Araque Caballero, M., Morenas-Rodríguez, E., Fellerer, K., Franzmeier, N., Kleinberger, G., Eren, E., Deming, Y., Piccio, L., Karch, C.M., Cruchaga, C., Paumier, K., Bateman, R.J., Fagan, A.M., Morris, J.C., Levin, J., Danek, A., Jucker, M., Masters, C.L., Rossor, M.N., Ringman, J.M., Shaw, L.M., Trojanowski, J.Q., Weiner, M., Ewers, M., Haass, C., 2018. CSF progranulin increases in the course of Alzheimer's disease and is associated with sTREM2, neurodegeneration and cognitive decline. EMBO Mol. Med. 10, e9712.
Takahashi, H., Klein, Z.A., Bhagat, S.M., Kaufman, A.C., Kostylev, M.A., Ikezu, T., Strittmatter, S.M., 2017. Opposing effects of progranulin deficiency on amyloid and tau pathologies via microglial TYROBP network. Acta Neuropathol. 133, 785–807.
Thal, D.R., Rüb, U., Orantes, M., Braak, H., 2002. Phases of Aβ-deposition in the human brain and its relevance for the development of AD. Neurology 58, 1791–1800.
Yin, F., Banerjee, R., Thomas, B., Zhou, P., Qian, L., Jia, T., Ma, X., Ma, Y., Iadecola, C., Beal, M.F., Nathan, C., Ding, A., 2010. Exaggerated inflammation, impaired host defense, and neuropathology in progranulin-deficient mice. J. Exp. Med. 207, 117–128.